AC-Corrosion and Electrical Equivalent Diagrams

L.V. Nielsen and P. Cohn***

*Department of Manufacturing Engineering
Materials Technology
Building 204
The Technical University of Denmark
DK – 2800 Lyngby, Denmark
e-mail: lvn@ipt.dtu.dk

**DONG - Natural Gas
The National Oil and Gas Company of Denmark
Agern Allé 24-26
DK – 2970 Hørsholm, Denmark
e-mail: pco@dong.dk

ABSTRACT

An electrical equivalent diagram representing the impedances existing between pipe and remote earth has been proposed for the purpose of modelling the AC-corrosion process. The diagram include static elements like soil- or spread resistance and the charge transfer resistance represented as Volmer-Butler exponential functions with some analogy to diodes. Dynamic elements, i.e. element with frequency dependant impedance, include diffusion (Warburg) impedances and capacitances. The characteristics of the Volmer-Butler function related to iron dissolution and re-depositions along with the DC offset conditions and amplitude of the AC-voltage cleaned from IR-drop is controlling the AC-corrosion rate. The spread resistance plays a major role in controlling the IR-free amplitude of the AC voltage.

KEYWORDS: AC corrosion, equivalent circuit elements, spread resistance, capacitance, diffusion, Volmer-Butler equation, diode analogies, corrosion rate

1. INTRODUCTION

Pipelines provided with high resistant coatings are susceptible to induction of AC voltage from e.g. paralleled high-voltage AC power lines. This AC-voltage may be a source of corrosion at coating defects where the AC current escapes the pipe. It is generally known that severe corrosion can result from AC, but – on the other hand - several pipelines are interfered with AC without experiencing corrosion problems. Yet the question is which conditions are provoking such AC corrosion attach and which conditions are not.

To a first approach, it seems plausible to consider electrical factors like the magnitude of the induced voltage (U_{AC}), the magnitude of the AC-current (I_{AC}) running to a coating defect (per unit area of the defect), or the level of CP supplied to the pipe. The latter comprises factors like the ON-potential (E_{ON}) of the pipe, the OFF-potential (E_{OFF}) of the pipe as well as the DC-current (I_{DC}) running to a coating defect (per unit area of the defect). However, these factors are interconnected by the chemistry and the physics of the soil surrounding the pipeline. Hence, the chemistry and the physics of the soil can be considered to be setting up some kind of elements that are equivalent to electrical elements.

The present paper encourages to setting up such equivalent circuits when dealing with AC corrosion, since they can be helpful in modelling the AC corrosion process, hence lead to a better understanding of the mechanisms behind AC corrosion. Since AC corrosion may not result from one single mechanism, several different equivalent circuits may be applicable, however, in this paper one circuit diagram is proposed, that seeks to comprise the physical and chemical aspects considered to be of relevance in an AC corrosion process.

2. PROPOSED ELECTRICAL EQUIVALENT CIRCUIT

The proposed circuit is schematically presented in figure 1. The electrical powers constitute a DC- and an AC source imposing a DC voltage and an AC voltage in between the pipeline and remote earth at specific location or coating defect. The AC source origins from the AC induction, whereas the DC source represents the cathodic protection system. The remaining part of the elements represent impedances relating to the physical and chemical factors existing in the current path from remote earth to a coating defect at the pipeline. In the following, these elements have been divided into static elements and dynamic elements as explained in further details below.

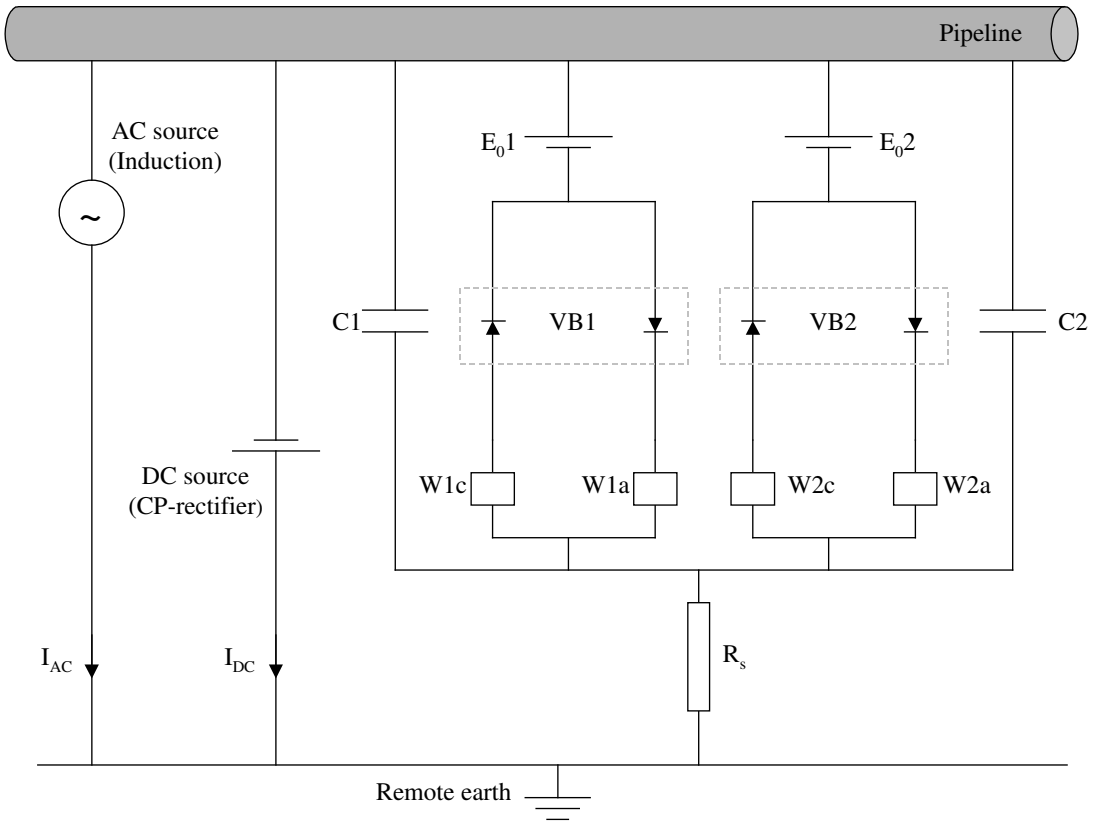

Figure 1. A schematic illustration of the electrical equivalent circuit proposed for AC-corrosion modelling.

2.1 Static Elements

The static elements are here defined as elements in which frequency has no direct influence on the impedance expressions. The soil resistance and the spread resistance, which are considered here as one single impedance element, is the first example of a static element. The second example is the charge-transfer impedance, that can be regarded as the basis for the perhaps more well-known polarisation resistance, which in this presentation is described as a function of the OFF-potential.

2.1.1 Soil Resistance – Spread Resistance (R_s)

The current flowing from remote earth to a coating defect of the pipeline runs through the soil, hence experiences the ohmic resistance provided by that soil (R_s in figure 1). Accordingly, IR drops relating to both DC and AC currents are set up. The ohmic resistance provided by the soil is controlled by factors relating to the resistance of the soil solution itself, the porosity of the soil, and – perhaps most important - geometrical factors existing close to the interface between the soil and the coating defect under consideration.

The resistance of the soil solution itself is inversely related to the conductivity of the solution. For ideal dilute solutions the conductivity of the solution may be calculated by:

$$\kappa = \sum_i C_i \cdot \lambda_i \qquad (1)$$

where C_i is the concentration of the ion i having equivalent molar ionic conductivity λ_i, proportional to the diffusion coefficient of that ion, D_i.

The porosity of the soil, p, is defined as the ratio between the volume of pores existing in the soil and the total volume of the soil. Assuming that the pores are filled up with soil solution with a certain conductivity, κ, and that the soil particles are non-conducting, the conductivity of the soil as a whole may be considered to be described in average by p multiplied with κ.

Concerning the geometrical factors, it is well recognised that the majority of the IR drop takes place in the very vicinity of the pipe to soil interface, i.e. at the coating defect. At this point the current flux lines concentrate causing a geometrical spread effect and associated spread resistance as illustrated in figure 2.

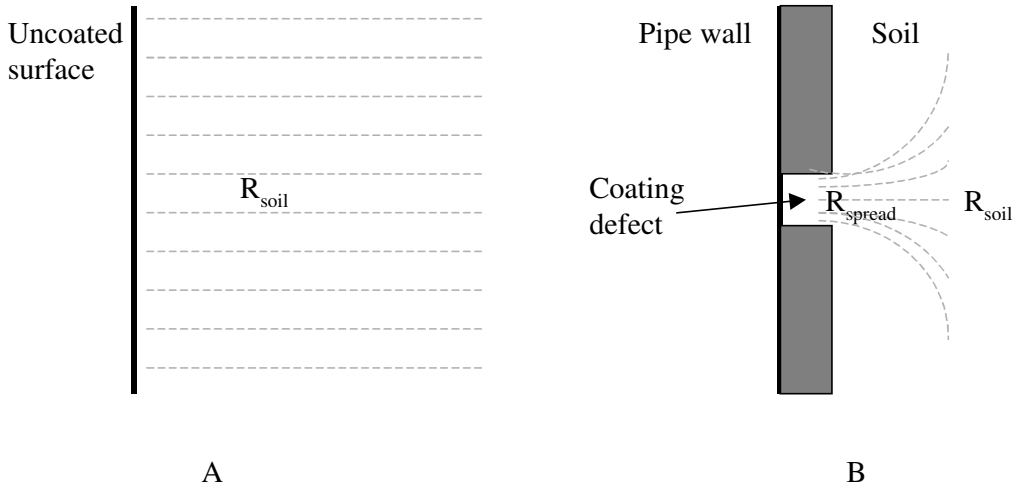

Figure 2. Illustration of geometrical effects on pipe to soil resistance.

The effect of electrode area on R_s has been studied previously using electrochemical impedance spectroscopy (EIS) measurements on steel electrodes with various areas exposed in an artificial soil solution.[1] Figure 3 shows the results of this investigation in terms of the normalised solution resistance ($\Omega.cm^2$) as a function of the applied electrode area.

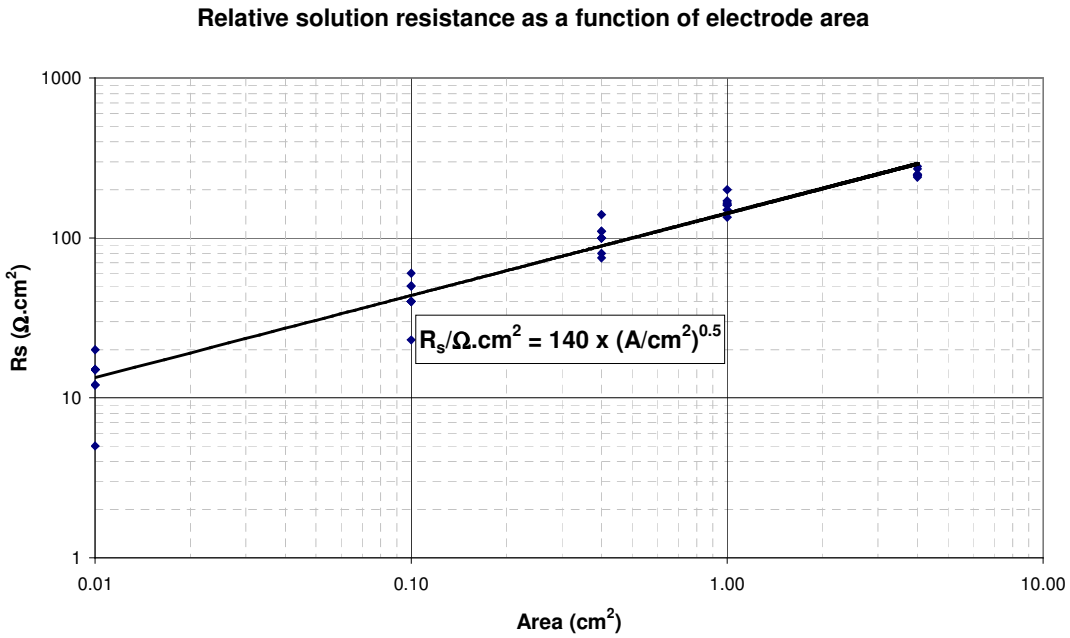

Figure 3. The relative solution resistance as a function of electrode area measured by EIS.[1]

In this case, the trend line suggests the following relation between measured R_s and electrode area:

$$R_s / \Omega \cdot cm^2 = 140 \cdot \sqrt{A / cm^2} \quad (2)$$

The expression may be generalised:

$$R_s = K \cdot \rho_s \cdot d \ \ (\Omega.m^2) \quad (3)$$

where K is a constant depending on the geometry of the defect, d is the extension of the defect, and ρ_s is the specific resistivity of the soil.

2.1.2 Charge Transfer – Diode Analogy (VB-Elements)

In the general case of DC-corrosion, the electrons released during anodic metal dissolution like iron oxidation:

$$Fe \rightarrow Fe^{2+} + 2e^- \quad (4)$$

are consumed by cathode reactions (reduction of hydrogen ions or oxygen):

$$2H^+ + 2e^- \rightarrow H_2 \quad (5)$$

$$O_2 + 2H_2O + 4e^- \rightarrow 4OH^- \quad (6)$$

Any electrochemical equilibrium existing at the steel surface defines an equilibrium potential E_0 associated to that particular equilibrium. Considering the general equilibrium:

$$aA = bB + ne^- \tag{7}$$

the associated equilibrium potential can be calculated according to the Nernst equation:

$$E_0 = E^0 + \frac{R \cdot T}{n \cdot F} \cdot \ln \frac{a_B^b}{a_A^a} \tag{8}$$

where E^0 is the standard equilibrium potential related to the electrode process and a_x is the activity or concentration of the species X.

At potentials different from the equilibrium potential, the process (7) will proceed with a velocity that can be described by the faradaic current according to the Volmer-Butler equation:

$$I_F = I_0 \cdot \left[\frac{C_{A,surface}}{C_{A,bilk}} \cdot \exp\left(\frac{E - E_0}{\beta_a} \right) - \frac{C_{B,surface}}{C_{B,bulk}} \cdot \exp\left(\frac{-(E - E_0)}{\beta_c} \right) \right] \tag{9}$$

I_F: Faradaic current related to the process,
I_0: Exchange current (faradaic in nature) related to the process,
$C_{i,\,surface}$: Surface concentration of species i,
$C_{i,bulk}$: Bulk concentration of species i,
E: Actual electrode potential, (E_{OFF} that is)
E_0: Equilibrium potential related to the process as given by the Nernst equation (15),
β_a, β_c: Tafel slope related to the anodic- and cathodic half cell reaction respectively.

Note that the Volmer-Butler equation relates to a single electrode equilibrium process, consisting of an anodic- and a cathodic branch having the individual current-potential characteristics (figure 4):

$$I_{F,a} = I_0 \cdot \left[\frac{C_{A,surface}}{C_{A,bulk}} \cdot \exp\left(\frac{(E - E_0)}{\beta_a} \right) \right] \tag{10}$$

$$I_{F,c} = I_0 \cdot \left[-\frac{C_{B,surface}}{C_{B,bulk}} \cdot \exp\left(\frac{-(E - E_0)}{\beta_c} \right) \right] \tag{11}$$

The following limes considerations can be extracted from those equations (with reference also to figure 4):

- When $E \rightarrow E_0$ then $I_{F,a} \rightarrow I_0$, and $I_{F,c} \rightarrow -I_0$,
- When $E \rightarrow \infty$ then $I_{F,a} \rightarrow \infty$, and $I_{F,c} \rightarrow 0$,
- When $E \rightarrow -\infty$ then $I_{F,a} \rightarrow 0$, and $I_{F,c} \rightarrow -\infty$,

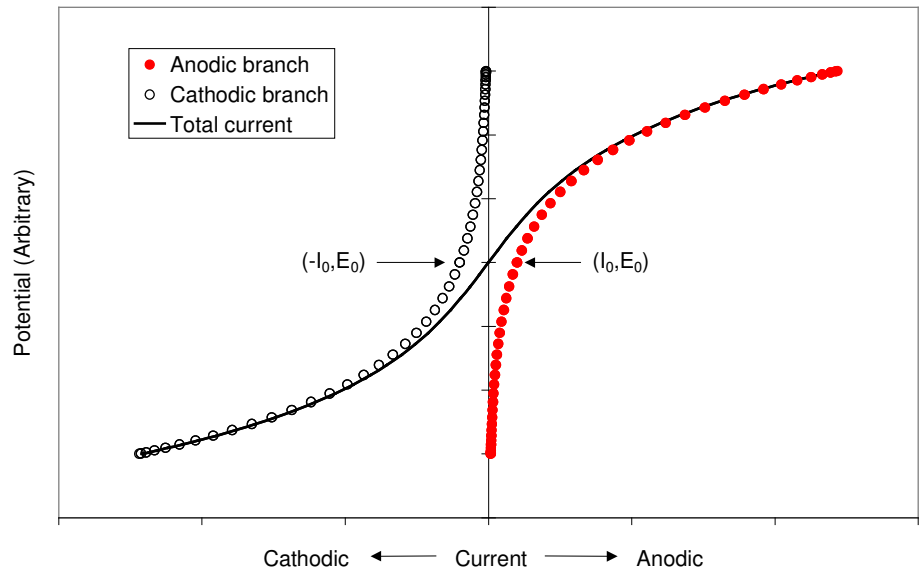

Figure 4. Illustration of the anodic- and cathodic branches of the Volmer-Butler equation and the summarised total current.

As observed, the individual branches (anodic/cathodic) of the Volmer-Butler equation can be described as exponential functions having a conducting voltage direction and an insulating voltage direction, hence may be ascribed some semi-conducting properties analogous to diodes. These directions oppose each other in the anode and the cathode branch. For this reason, each electrochemical equilibrium process participating in the AC-corrosion event is presented in the electrical equivalent circuit diagram as two opposed diodes with potential-current characteristics as given by equations (10) and (11). In figure 1, two such processes have been included (VB1 and VB2), one of which representing the metal dissolution and reversed metal re-deposition, the other representing a typical cathode process like reduction of hydrogen ions (5) or reduction of oxygen (6). Figure 5 shows schematically in an E-log(I) plot two Volmer-Butler processes and their summation (the summation being the actual faradaic current flowing at the respective potential, which at $I_F = 0$ defines the open circuit potential, (OCP) resulting from a sinusoidal voltage oscillation with a certain period Δt (say 20 ms corresponding 50 Hz).

The charge Q_i released by the individual or summarised processes during time t may be calculated by:

$$Q_i(t) = \int_0^t I_i \cdot dt \tag{12}$$

whereas the faradaic current related to the individual process i within one cycle having period Δt can be calculated by:

$$I_i(\Delta t) = \frac{\Delta Q_i}{\Delta t} \tag{13}$$

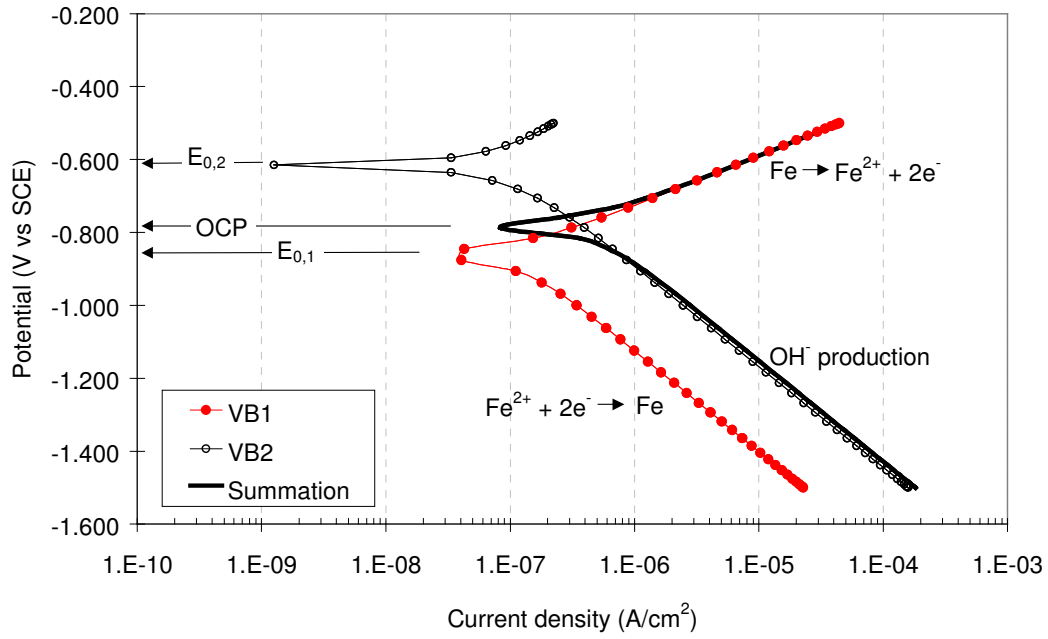

Figure 5. Example of E-log(I) behaviour of two Volmer-Butler processes and their summation (applied values: VB1: I_0 = 1.1 x10^{-7}A/cm^2, E_0 = -0.86V, βa = 0.06V/decade, βc = 0.12V/decade, VB2: I_0 = 1.0x10^{-7}A/cm^2, E_0 = -0.615V, βa = βc = 0.12 V/decade, sinusoidal potential variation with offset = -1.0V and amplitude = 0.5V. Surface concentration equals bulk concentration.

Using equation (13) on the VB1 process (metallic dissolution and re-deposition), the instant corrosion rate can be calculated according to usual correlations between dissolution current density and corrosion rate. Also, using the same equation on the VB2 process, the rate of production of alkalinity can be calculated, and using the equation on the sum of VB1 and VB2, the apparent DC current can be calculated. In the above example, the resulting DC current is –2.85 µA/cm^2 (cathodic that is), the resulting rate of production of alkalinity corresponds –3.65 µA/cm^2, whereas the dissolution current density is 0.8 mA/cm^2 corresponding a corrosion rate of 9.3 µm/year. Naturally, these figures are under the assumption that the employed set of conditions (amplitude, exchange currents, Tafel slopes etc.) does not change with time.

2.2 Dynamic Elements

In this presentation, the dynamic elements are elements with frequency-dependant impedance expressions. These include interfacial capacitance and diffusion elements.

2.2.1 Interfacial Capacitance (C)

The corrosion process implies that positively charged ions are dissolved in solution, whereas the excess electrons initially are accumulated in the steel-lattice. The accumulation of negative charge in the steel surface attracts positively charged ions from the electrolyte. The net result is a build-up of an electronegative front in the steel surface facing an electropositive front in the electrolyte (figure 6).

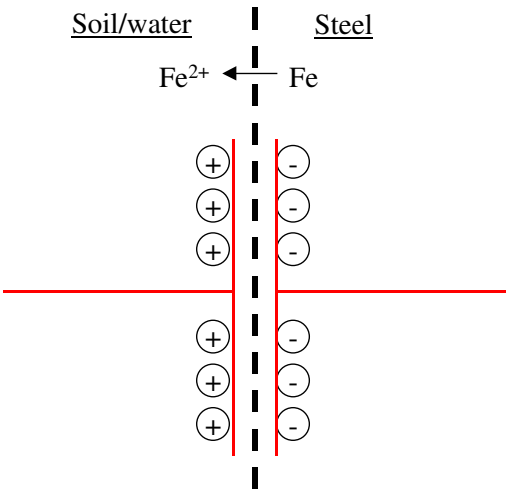

Figure 6. Schematic presentation of the steel-water interface acting as a capacitor due to specific set-up of negative and positive charge across the interface.

Hence, due to this charge arrangement, the interface acts as a capacitor, and the capacitance that can be associated to the interface is known as the double layer capacitance, C_{dl}. A capacitor is defined as an element in which the current in the element is the time derivative of the voltage and the voltage is a function of the current integrated over time:

$$I = C \cdot \frac{dU}{dt} \quad \Rightarrow \quad U = \frac{1}{C} \cdot \int I\,dt + k \tag{14}$$

The impedance of a capacitor can be described by:

$$Z_C = \frac{1}{2 \cdot \pi \cdot f \cdot C} \tag{15}$$

where f denotes the applied frequency and C denotes the capacitance of the capacitor. As observed, the impedance of the double layer capacitance depends on applied frequency:

$$f \to \infty \Rightarrow Z_{Cdl} \to 0 \text{ and } f \to 0 \Rightarrow Z_{Cdl} \to \infty \tag{16}$$

The capacitance of a plate capacitor can be described by:

$$C = \varepsilon \cdot \frac{A}{d} \tag{17}$$

where A is the area of the plates, d is the distance between the plates, and ε is the dielectric constant of the dielectricum positioned in between the plates.

In connection to corrosion processes, a capacitor may be associated to any interface existing at the corroding interface. This may be the double layer or any films covering the surface.

2.2.2 Diffusion (W-Elements)

Diffusion is defined as a random movement of species causing a flux of the species downhill a concentration gradient. Whenever such concentration gradient exists, diffusion occurs. Dealing with a coating defect, at which species are consumed or produced, the species diffuse in the direction with the lowest concentration. Regarding cathodically protected steel, the cathodic polarisation of the steel causes a displacement of the pH in the direction of alkalinity (rising pH), since the CP initiates cathode reactions like reduction of acid (5) or reduction of oxygen (6). As observed from these equations, acid (H^+) is consumed or alkalinity (OH^-) produced both causing a rise in pH corresponding a direct proportionality between the DC-current flow (e^-) and the produced equivalent of alkalinity. Since these reactions take place directly at the steel surface, this sets up a pH gradient (H^+ concentration gradient) in the proximity of the surface, and consequently diffusion processes initiate. Hence, diffusion processes renew H^+ at the cathodically protected surface, whereas OH^- diffuses away from the surface, both causing a moderation of the pH increase otherwise taking place at the surface.

The same scenario sets up when steel is corroding according to equation (4). In this case Fe^{2+} ions diffuses away from the surface.

Ficks' laws of diffusion determine the rate by which diffusion occurs:

$$1^{st}\text{ law of diffusion}: \qquad J_i = -D_i \cdot \frac{\delta C_i}{\delta x} \tag{18}$$

$$2^{nd}\text{ law of diffusion}: \qquad \frac{\delta C_i(x,t)}{\delta t} = D_i \cdot \frac{\delta^2 C_i(x,t)}{\delta x^2} \tag{19}$$

The first law states that the flux of the diffusing species J_i is proportional to the concentration gradient $\delta C_i/\delta x$, with the proportionality factor D_i (diffusion coefficient D_i). Note the analogy to Ohm's law (J_i ~ current I, $\delta C_i/\delta x$ ~ voltage U, and D_i ~ inverse resistance 1/R). The second law takes into account the effect of time changing gradients.

In figure 1, the diffusion element has been implemented as a Warburg impedance element, W, which is known from general electrochemical modelling. The magnitude of the impedance Z_D of such diffusion element can be described by the generic expression (originally a complex impedance with symmetrical coefficients):[2]

$$Z_D = \frac{\sigma}{\sqrt{\pi \cdot f}} \tag{20}$$

where σ, the Warburg coefficient is given by:

$$\sigma = \frac{R \cdot T}{n^2 \cdot F^2 \cdot A \cdot \sqrt{2}} \cdot \left(\frac{1}{C_{O,bulk} \cdot \sqrt{D_O}} + \frac{1}{C_{R,bulk} \cdot \sqrt{D_R}} \right) \tag{21}$$

R is the gas constant, T is temperature, n is number of electrons involved in the electrochemical process, F is Faraday's number, A is the area (of the coating defect), $C_{O,bulk}$

and $C_{R,bulk}$ is the bulk concentration of oxidant and reductant respectively, and D_O and D_R is related diffusion coefficients.

3. DISCUSSION

The key element of the AC-corrosion process is the VB1 element (figure 1) describing the iron dissolution and re-deposition characteristics. If the offset conditions along with the characteristics of the individual anode and cathode process (equations (10) and (11)) of VB1 are balanced so that (with reference to equation (13):

$$I_a(\Delta t) > I_c(\Delta t) \quad \Rightarrow \quad \frac{\Delta Q_a}{\Delta t} > \frac{\Delta Q_c}{\Delta t} \tag{22}$$

then AC-corrosion occurs. If opposite, then AC corrosion does not occur. Equation (22) simply states that if – during a single cycle of AC – the anodic charge released due to iron dissolution exceeds the cathodic charge released due to re-deposition of dissolved iron, then corrosion occurs. In the following, the influence of the single elements on mainly the VB1 characteristics will be examined more closely.

3.1 Effect of Spread Resistance

Equations (2) and (3) relating to the spread resistance have important influence on the offset conditions. Firstly, R_s determines the amount of AC-voltage being lost across the soil resistance (magnitude of the IR drop related to the AC voltage). This means that if R_s is very high, a high degree of the AC voltage is lost across the soil resistance thus degreasing the amount of AC voltage reaching the pipe, and vice versa. Secondly, the size of the coating defect has a major influence on R_s in the sense that small defects produce small R_s values whereas larger defects produce larger R_s values (the latter being beneficial in inhibiting AC-corrosion). Thirdly, the specific resistance of the soil ρ_s refers to the resistance of the soil present at the very vicinity of the coating defect. This means that – depending on the modification of the soil chemistry at the coating defect caused by the AC and DC voltage – the soil resistance may increase, it may be unaffected, or it may decrease throughout time.

The chemistry formed in the vicinity of the steel-soil interface and the resistance formed in conjunction herewith is the basis for a mechanism of AC corrosion proposed by Stalder et al.[3,4] This takes into consideration the ratio between earth alkaline and alkaline cations present in the soil and the hydroxides and carbonates accordingly formed. Earth alkaline cations like calcium and magnesium forms hydroxides ($Ca(OH)_2$, $Mg(OH)_2$) caused by alkalisation of the environment due to the CP (the appearance of very high pH is claimed to be usual). Under influence of CO_2, these hydroxides may be converted into carbonates ($CaCO_3$, $MgCO_3$). Both hydroxides and carbonates of earth alkaline cations are solids with quite weak dissolvability. In contrast, hydroxides of alkaline cations like sodium and potassium (NaOH, KOH, Na_2CO_3, K_2CO_3), are quite dissolvable, i.e. they do not form solid precipitates as easy as does the earth alkaline cations. Solid precipitates in general are expected to increase R_s. Hence, the presence of earth alkaline cations in combination with a pH increase caused by well-functioning CP is expected to increase R_s. The case of absence of earth alkaline cations (cations present as alkaline – not earth alkaline cations) does not lead to this increase in R_s. In other words, the formation of high resistive deposits depends on the presence of earth alkaline cations in the

soil. If resistive deposits are formed, R_s increases, yet allowing increasingly less AC-current to reach the pipe at a coating defect. The absence of earth alkaline cations means that no such resistive precipitates are formed, hence, the amount of AC-current reaching the pipe is not limited and AC-corrosion can proceed. One important parameter of the thesis is then the ratio between concentration of earth alkaline cations and alkaline cations present in the soil.

This can be put in perspective of the present model. Simple polarisation experiments have shown[5] that earth alkaline cations passivates the anodic branch of the metal dissolution (VB1) process at pH values as low as around 6, i.e. with reference to figure 5, a constant very low anodic current is present. Alkaline cations do not have the same passivating capability. A certain critical mixture of earth alkaline and alkaline cations defines whether the steel passivates or not. Regardless of the electrolyte composition, at higher pH, the steel passivates whereas at very high pH values, the steel re-activates as illustrated in the Pourbaix-diagram, figure 6.

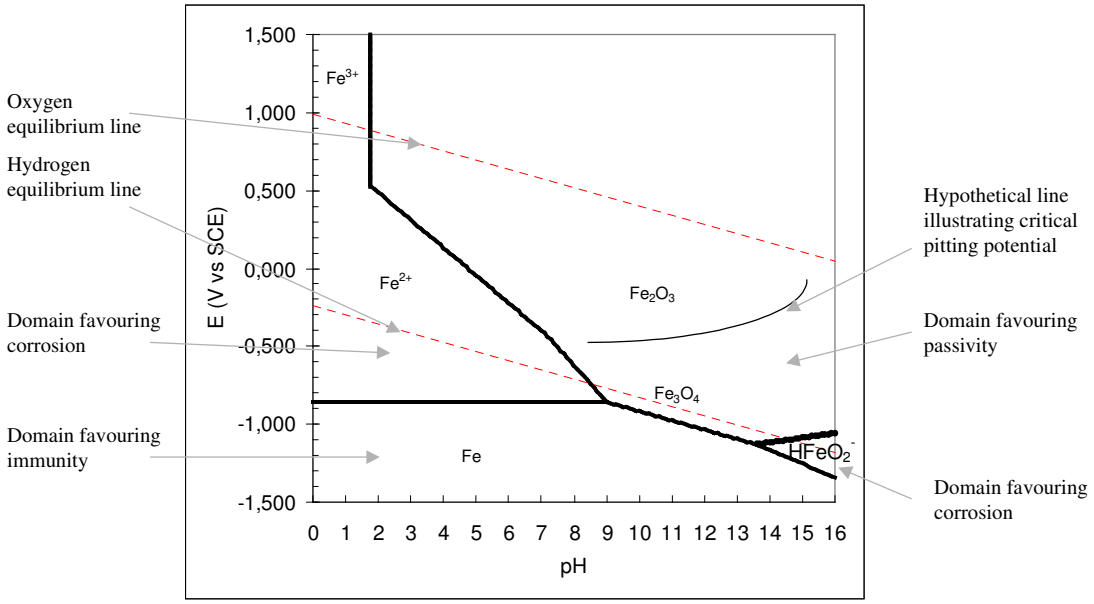

Figure 6. Pourbaix-diagram showing domains of corrosion passivity and immunity as a function of pH and potential. Based on Pourbaix-atlas.[6]

A further aspect of the spread resistance may include the distinct tubercle of "stone hard soil" (comprising corrosion products etc.) that is frequently observed to grow from the coating defect in connection with AC-corrosion incidents (schematic illustration in figure 7). The specific resistivity of such tubercle is expected to be distinctively lower than the specific resistivity of the surrounding soil, in other words, the chemistry nearby the coating defect has changed from higher to lower resistive substances. In addition, the surface area of the tubercle is considerably higher than the area of the original coating defect, hence, the current flux to the pipe at the coating defect can spread out using the entire area of the tubercle before entering the pipe. Accordingly, R_s is expected to be dramatically decreased during the corrosion process, both caused by the exchange of the chemistry in the vicinity of the coating defect and by the enhanced area available for current donation. Consequently, the growth of such tubercles may escort an autocatalytic corrosion attack.

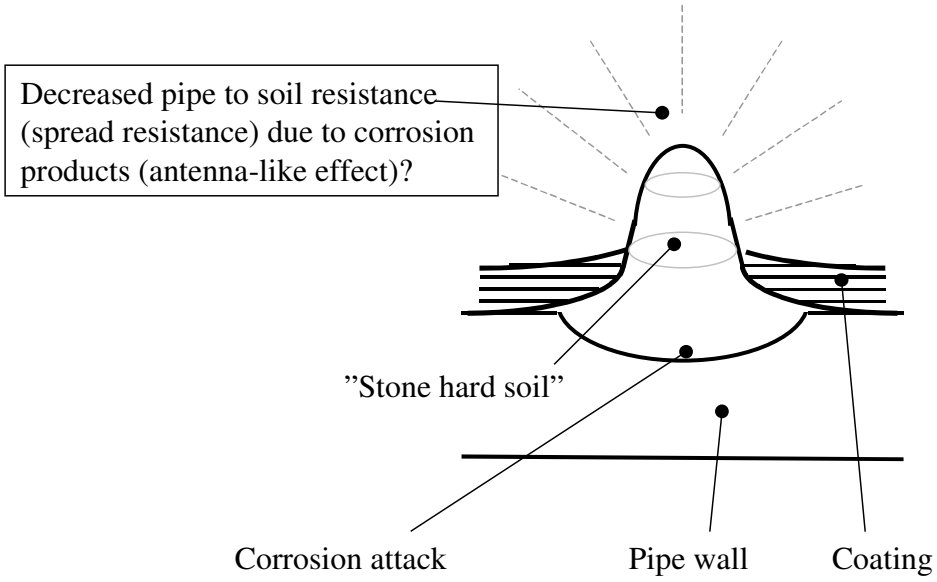

Figure 7. Schematic illustration of a tubercle of “stone hard soil” that frequently has been observed to grow from the coating defect in connection with AC-corrosion incidents.

The effect of the spread resistance on the AC-corrosion rate may be illustrated with reference to figure 8. Here the spread resistance has been considered to change over time whereby the AC peak potentials actually reaching the pipe (i.e. the off-potentials) changes according to an exponential function:

$$U_{AC\text{-}pp,OFF}(t) = U_{AC\text{-}pp,OFF}(t = 0) \cdot \exp(a \cdot t) \qquad (23)$$

In this equation, a is some characteristic constant. Two examples have been presented in figure 8. One example illustrates what happens if the spread resistance increases (the constant a chosen as -10^6 in equation (23)), the other example illustrates what happens if the spread resistance decreases (the constant a chosen as 10^6). In both cases, the conditions represented in figure 5 have been applied, and the corrosion rate calculated using equation (13) with equal bulk and surface concentrations (no diffusion limitation). In figure 8, the corrosion rate and the amplitude of the AC voltage in the off-condition has been shown. The time t is actually in seconds, however illustrated as a dimensionless parameter.

As observed from the figure, one may establish a certain incubation time prior to which neither the amplitude nor the corrosion rate (being close to zero) changes considerably. After this incubation time, if the spread resistance increases i.e. the amplitude decreases, then the corrosion rate decreases as well (actually it becomes negative, which just indicate the Fe^{2+} ions will precipitate), whereas a decrease in spread resistance (increase in amplitude) leads to an increase in corrosion rate. In both of these cases, the DC current stays cathodic (20-40 $\mu A/cm^2$), and therefore this should not be taken as a measure that no corrosion occurs.

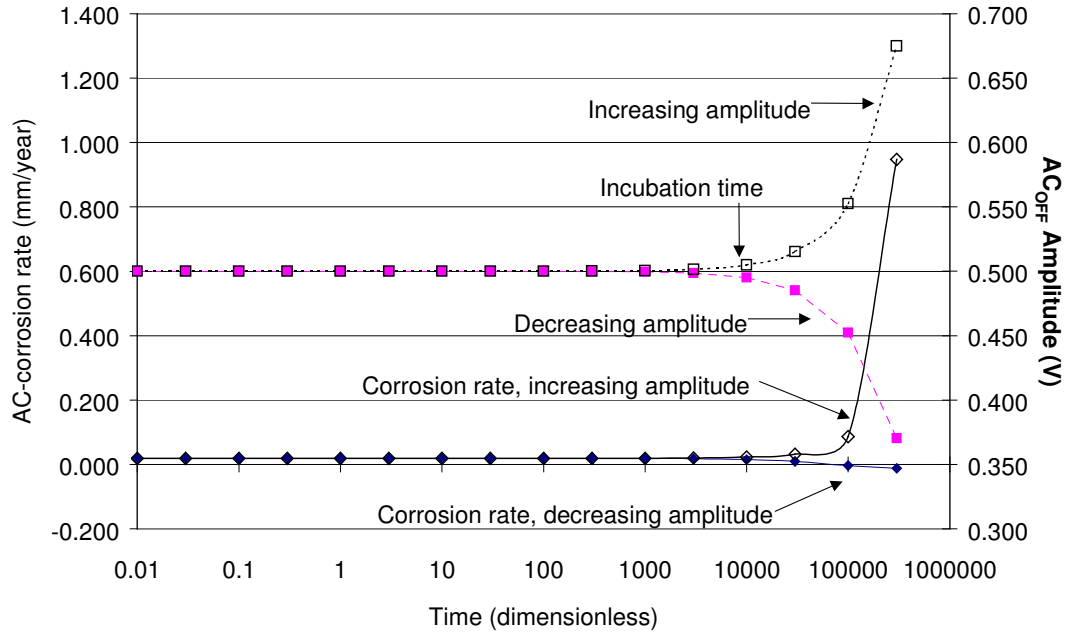

Figure 8. Calculated corrosion rate as a function of time when spread resistance decrease or increase.

3.2 Effect of Diffusion

Firstly, it is noted that the Warburg coefficient (equation (21)) is inversely related to the surface area. Consequently the diffusion impedance (equation (20)) is inversely related to the area as well, i.e. diffusion is accelerated with decreasing area of the coating defect. Note as well that the Warburg impedance relates only to infinite diffusion, i.e. diffusion in which the possible extension of the diffusion layer is not limited, but this is a quite good approximation when dealing with diffusion in soil.

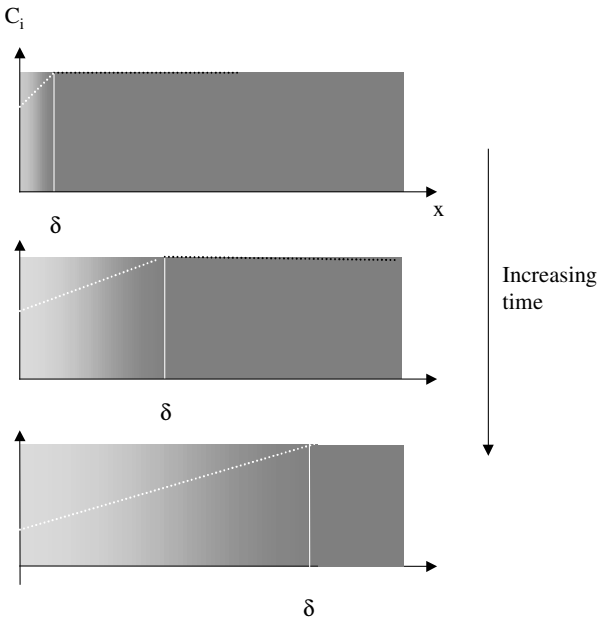

Figure 9. Schematic illustration of the concentration gradient across the diffusion layer. The diffusion layer distance as well as the surface concentration (C_i at $x = 0$) may vary with time.

Referring to equation (18), the flux of species related to diffusion is proportional to the difference in concentration existing across the diffusion layer, but inversely proportional to the extension or thickness of the diffusion layer. The distance δ (thickness of diffusion layer) over which the concentration difference exist may vary with time as illustrated in figure 9. Also, the surface concentration may change throughout time.

Partly derived from the diffusion equations (18) and (19), the thickness of the diffusion layer δ under steady state (DC) conditions is a function of time and the diffusion:[2]

$$\delta(t) = \sqrt{\pi \cdot D \cdot t} \tag{24}$$

Experiments involving a cathodically protected steel surface submerged in an artificial soil solution suspended in sand have shown[7] that the rate by which an alkaline front moves away from the protected surface defines a diffusion coefficient for H^+ in that suspension in the order 3.4 x 10^{-4} cm^2/sec. (tabulated values are in the order of 9 x 10^{-5} cm^2/sec (H^+ in weak acid[8]) hence the measured value may be surprisingly high).

Under alternating conditions e.g. brought about by an AC voltage having frequency f, the extension of the diffusion layer d can be described as a function of the diffusion coefficient D and the applied frequency:[2]

$$\delta(f) = \sqrt{\frac{\pi \cdot D}{2 \cdot f}} \tag{25}$$

When comparing equation (24) and (25) one important aspect is that the thickness of the diffusion layer is considerably larger in a pure DC condition (24) than the thickness under say 50 Hz AC (25). Using the measured diffusion coefficient as an example, the thickness of the diffusion layer as a function of time becomes:

$$\delta / \text{cm} = 1.97 \cdot \sqrt{t / \text{hours})} \tag{26}$$

This equation shows e.g. that after only 24 hours, the diffusion layer (the extension of the zone being chemically affected by CP) reaches 10 cm out into the bulk of the soil. In comparison, during a 50 Hz AC cycle, the extension of the diffusion layer is in the order of μm. In other words, during one single cycle of AC, the diffusion limitation is very modest and may be disregarded in comparison with the limiting (or modifying) effects of diffusion under long-term DC influence. This means that terms like thickness of the diffusion layer and surface versus bulk concentration are different in the DC (long term) and in the AC (short term; within one cycle) situation. If one could record exclusively the faradaic current within one cycle of AC simultaneously with the off-potential, one would expect a quite perfect charge transfer controlled Volmer-Butler curve with no effect of diffusion. The bulk concentration of the involved species would approach the surface concentration.

However, due to a rectification or a DC offset that causes a certain DC current to flow throughout time, the bulk versus surface concentration (appearing in the Volmer-Butler equation (16)) and the extension of the diffusion affected zone (as defined in figure 9) becomes important. Still, the fact that diffusion is not a limiting parameter within one cycle of AC, the faradaic current as described by a Volmer-Butler becomes a very good approximation. Throughout time however, the elements enclosed in the Volmer-Butler

equation may change due to diffusion processes. In particular, this relates to exchange current density and equilibrium potentials whereas ratio between surface versus bulk concentration of involved species is expected to be around 1 even though the actual concentrations may change.

As an illustration of how the diffusion processes affect the AC-corrosion process, consider the Fe^{2+} surface concentration throughout time:

$$C_{Fe^{2+}}(t) = C_{Fe^{2+}}(t=0) + n_1 \cdot F \cdot I_{F,VB1} \cdot t - \sqrt{\pi \cdot D_{Fe^{2+}} \cdot t} \tag{27}$$

The first term refers to initial iron concentration, the second term relates to production of Fe^{2+} according to equation (12) and the third term relates to diffusion of Fe^{2+} away from the surface using a generic expression similar to (24). The equation (27) arises from simple mass balance considerations. Hence, depending on the magnitude of the faradaic current related to ferrous iron production ($I_{F,VB1}$) and the diffusion coefficient for ferrous iron diffusion (D_{Fe2+}), the surface concentration of ferrous iron may increase, decrease or by coincidence remain undisturbed. Now, considering for example the conditions outlined in figure 5, it is clear that for a certain offset DC-potential and a certain fixed amplitude of the AC voltage reaching the pipe (AC_{OFF}) the equilibrium potential related to the VB1 process has to decrease in order to accelerate corrosion. According to the Nernst equation (15), the surface concentration of ferrous irons (Fe^{2+}) has to decrease in order to fulfil this requirement. Accordingly, by viewing equation (27) this condition is achieved only when:

$$n_1 \cdot F \cdot I_{F,VB1} \cdot t < \sqrt{\pi \cdot D_{Fe^{2+}} \cdot t} \tag{28}$$

Since also the corrosion rate is directly proportional to $I_{F,VB1}$, the maximum corrosion rate (corrosion current density) as a function of time can be derived as:

$$I_{F,VB1MAX}(t) = \frac{\sqrt{\pi \cdot D_{Fe^{2+}}}}{n_1 \cdot F \cdot \sqrt{t}} \tag{29}$$

Equation (29) shows that the maximum corrosion rate decreases throughout time and necessarily leads to the quite important conclusion that diffusion processes alone cannot modify the Volmer-Butler processes in such a manner that accelerating corrosion sets up. If the ferrous iron produced by corrosion is bound up in solid substances, complex species or ions different from the Fe^{2+} ion just as soon as it is produced at the surface, the achievement of a combined condition of a decreasing surface concentration of Fe^{2+} and accelerated corrosion may be accomplished.

In the electrical equivalent model (figure 1) 4 diffusion (Warburg) elements have been incorporated. This is to point out that diffusion processes are involved in any of the “diodes” or individual branches of the VB-processes that occurs in the AC-corrosion scenario.

3.3 Effect of the Characteristics of the VB-Element

For the general process (7), the rate of the forward reaction V_+ and the rate of the backward reaction V_- can be described by

$$V_+ = k_+ \cdot [A]^a, \qquad V_- = k_- \cdot [B]^b \tag{30}$$

where k_+ and k_- are the rate constants associated with the forward and backward reaction respectively. It is clear that a time constant can be associated to any chemical process, since a chemical process involves a change in the arrangement of the elementary physics of the involved species. If the driving force for the process is present only for a short but repeated period of time like e.g. during the anodic half cycle of a sine wave, it is clear that integrated over time, a smaller fraction of the species participating in the process will react. One way of expressing this may be to look upon the rate constant of the process as a factor that includes the process time constant. Hereby, the rate constant becomes frequency dependant, and since the time constant of the processes depends largely on the chemical and physical conditions at the surface, this constant is likely to may change with time. The Volmer-Butler equation (16) is derived using the usual bond between the rate constant and electrode potential:[9]

$$\begin{aligned} k_+ &= k_+^0 \cdot \exp\left[(1-\alpha)\cdot(E_0 - E^0)\cdot\frac{n\cdot F}{R\cdot T}\right] \\ k_- &= k_-^0 \cdot \exp\left[-\alpha\cdot(E_0 - E^0)\cdot\frac{n\cdot F}{R\cdot T}\right] \end{aligned} \tag{31}$$

where α is the charge transfer coefficient and K^0 is the standard rate constant from where the exchange current density I_0 is derived. Comparing with the Volmer-Butler equation (16) it is acknowledged that changes in the rate constants of the involved processes can be implemented in the Volmer-Butler equation as changes in both the Tafel slopes and in the exchange current densities.

As an example based on the initial conditions presented in figure 5, the corrosion rate versus cathodic Tafel slope of the VB1 process in figure 5 is illustrated in figure 10. The condition of increasing Tafel slope with time reflects an inhibition of the iron precipitation process, and a large Tafel slope (say 10) reflects that some maximum current can be released during the cathodic part of the VB1 process. In this case, the corrosion rate is at maximum for this particular set of conditions, and this maximum level reflects the total amount of charge available in the anodic branch of the VB1 process.

In a similar manner, the corrosion rate is sensitive to changes in the exchange current density if the VB1 process as illustrated in figure 11. The effect is more pronounced in comparison with the effect of an increasing Tafel slope that has a limit value conducted by the charge included in the anodic branch of the process.

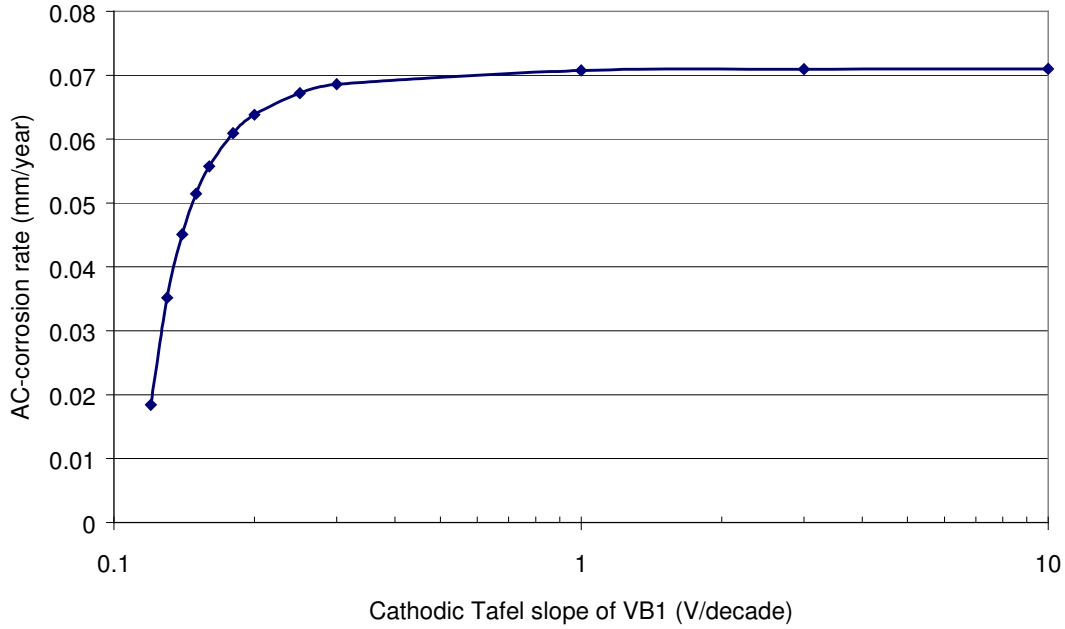

Figure 10.Effect of increasing cathodic Tafel slope on AC-corrosion rate.

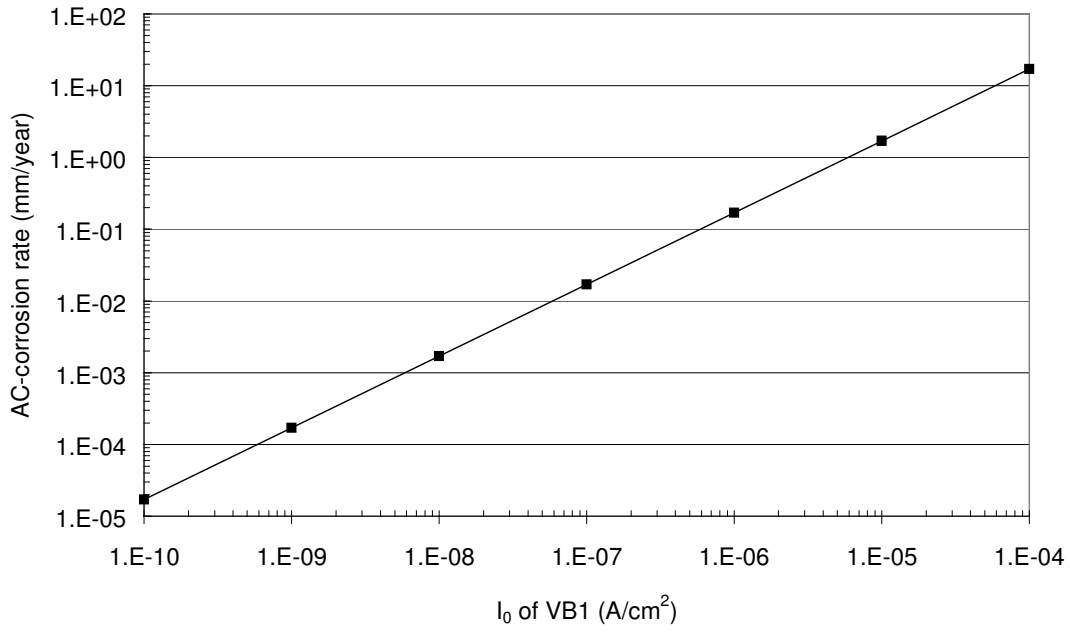

Figure 11. Effect of exchange current density of VB1 process on corrosion rate.

3.4 Effect of Capacitance

In figure 1, two capacitors have been implemented in the model. C1 is connected as an alternative current path relative to the current running trough the VB1 process, whereas C2 is connected similarly in parallel with the VB2 process. In the mathematical sense, these could have been regarded as one, having C1 + C2 as capacitance, but they are here split up to indicate that the specific set up of charge shown in figure 6 can result from both anodic

dissolution as well as cathode processes. In the following, they are however treated as one capacitor.

As observed from equation (17) the capacitance increases when the area of the plates increases (this may be realised in the corrosion process by enhancing the surface area due to corrosion or by introduction of porous corrosion product layers etc.). In turn, this means that the impedance of the capacitor decreases allowing for a certain AC voltage an increased amount of AC-current to pass. The same occurs if the distance between the plates increases, and this distance can be regarded as the distance between the arrays of the positive and negative charge, or – in connection with surface covering films - the thickness of the film. Further, the dielectricum properties may have similar influence.

It should be stressed out that since the specific arrangement of ions across the steel-water interface is highly dependent on potential and pH, so is the magnitude of the capacitance. Since also the degree of deposits covering the surface is strongly dependent on both potential and pH, so is the magnitude of the capacitance associated to film processes.

In any case, the net result of the overall capacitance effect is that the capacitors act as a drain for AC current. In figure 1, the capacitors have been placed in parallel with the elements through which the faradaic current passes i.e. in parallel with the elements accounting for the behaviour of the chemical and electrochemical kinetics. Supposing that these elements in all can be replaced with an element having impedance Z_F, then the current division between the Z_F element and the capacitor having impedance Z_C according to equation (15) can be loosely described by (phases disregarded):

$$I_{Total} = I_F + I_C = \frac{U_{AC,OFF}}{Z_F} + \frac{U_{AC,OFF}}{Z_C} \tag{32}$$

In this equation, $U_{AC,OFF}$ is the total AC voltage subtracted by the IR-drop existing across R_s. According to equation (32), the efficiency of the draining effect of the capacitor P can be expressed as:

$$P = \frac{Z_F}{Z_C + Z_F} \qquad (P \to 1 \text{ when } Z_C \to 0 \text{ and } P \to 0 \text{ when } Z_C \to \infty) \tag{33}$$

Consequently the draining effect of the capacitor is very much dependant on the magnitudes of the faradaic impedances. However, if $Z_F >> Z_C$ then the draining effect is very high, and only a small fraction of the total current is faradaic in nature causing only a small phase between voltage and current. Since the faradaic current cover both dissolution and re-deposition as well as acid consumption and production, the amount of current actually causing the corrosion is expected to be just a small fraction of the total AC current. Figure 12 shows result from experiments where the corrosion rate of cathodically polarised steel superimposed with various levels of AC current have been measured using a high-sensitive electrical resistance based technique.[10] The fractions (percent) of the total current actually causing corrosion has been noted in some of the data points for information. Note that the corrosion indicated in figure 12 decayed over time.

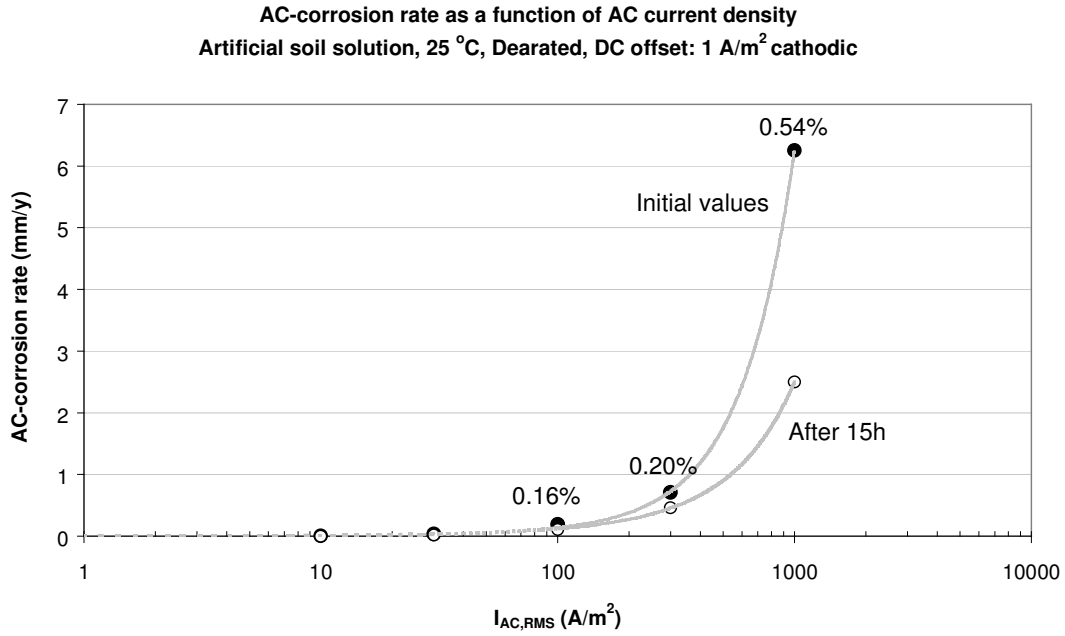

Figure 12. Effect of AC current density on corrosion rate of cathodically polarised steel exposed in artificial soil solution.[10]

4. CONCLUSIONS

An electrical equivalent diagram representing the impedances existing between pipe and remote earth has been proposed for the purpose of modelling the AC-corrosion process. The diagram include static elements like soil- or spread resistance and the charge transfer resistance represented as Volmer-Butler exponential functions with some analogy to diodes. Dynamic elements, i.e. element with frequency dependant impedance, include diffusion (Warburg) impedances and capacitances. The characteristics of the Volmer-Butler function related to iron dissolution and re-depositions along with the DC offset conditions and amplitude of the AC-voltage cleaned from IR-drop is controlling the AC-corrosion rate. The spread resistance plays a major role in controlling the IR-free amplitude of the AC voltage.

5. REFERENCES

1. Electrochemical Impedance Spectroscopy (EIS) Investigation of the Randles Circuit Elements for Carbon Steel Exposed in Artificial Soil Solution: Effect of Electrode Area and DC-Offset Potential, L.V. Nielsen ("Notes on"- series, Project: AC-Corrosion Sponsored by the National Oil and Gas Company of Denmark). The Technical University of Denmark, 1999.

2. Physical Interpretation of the Warburg Impedance, S.R. Taylor and E. Gileady, CORROSION 51, (9), pp. 664-671, (1995).

3. Stalder in Draft CEOCOR Booklet on AC Corrosion on Cathodically Protected Pipelines

4. Influence of Soil Composition on the Spread Resistance and of AC-Corrosion on Cathodically Protected Coupons. C.H.Voûte, This Congress.

5. Polarisation Behaviour of Steel Exposed in Various Mixtures of Alkaline- and Earth Alkaline Cations, L.V. Nielsen ("Notes on"- series, Project: AC-Corrosion Sponsored by the National Oil and Gas Company of Denmark). The Technical University of Denmark, 1999.

6. M. Pourbaix, Atlas of Electrochemical Equilibria in Aqueous Solutions, NACE/CEBELCOR, 1974.

7. Potential- and pH Gradients Existing in Proximity of Cathodically Protected Steel Buried in Sediment, L.V. Nielsen ("Notes on"- series, Project: AC-Corrosion, Sponsored by the National Oil and Gas Company of Denmark). The Technical University of Denmark, 1999.

8. Handbook of Chemistry and Physics, 75th edition, D.R. Lide (Ed.), CRC Press, 1995

9. K.J. Vetter, Electrochemical Kinetics, Academic Press, New York/London, 1967

10. AC-Corrosion Rates of Cathodically Polarised Steel in Artificial Soil Solution, L.V. Nielsen ("Notes on"- series, Project: AC-Corrosion, Sponsored by the National Oil and Gas Company of Denmark). The Technical University of Denmark, 2000.